Correlated Sampling With Application to Carrier Power Estimation Accuracy

J. R. Lesh
DSIF Operations Section

In this article the total sampling time and number of samples required to produce a sample mean having a specified variance is evaluated for various sampling intervals. The samples are assumed to be the correlated outputs of either a first- or second-order system having a white gaussian noise input. It is found that a reduction in both the total time and the number of samples can often be obtained for a given variance and sampling interval if the sampling is performed at the output of a second order system. These results are then applied to the automatic gain control sampling presently being used for carrier power estimation to show how its accuracy can be improved.

I. Introduction

It is a well-known result that the variance of the sample mean of a random process (σ_M^2) is related to the variance of the process itself (σ^2) by

$$\sigma_M^2 = \frac{1}{N}\sigma^2 \tag{1}$$

(where N is the number of samples) provided each of the samples is uncorrelated with all of the others. However, in practice the time required to obtain N independent samples (for large N) may become so large as to make it impractical. For such cases, correlated sampling must be performed.

When a sample mean is compiled from correlated samples the conditions necessary for Eq. (1) to hold are violated. Davenport and Root (Ref. 1) considered this problem and derived the relationship

$$\frac{\sigma_M^2}{\sigma^2} = \frac{1}{N} + \frac{2}{N}\sum_{k=1}^{N-1}\left(1 - \frac{k}{N}\right)\widetilde{R}(kt_0) \tag{2}$$

where $\widetilde{R}(t)$ is the normalized covariance function of the process and t_0 is the sampling interval. Unfortunately, solution of this equation for N (or equivalently the total time $T = Nt_0$) becomes exceedingly difficult for even moderately small given vaues of σ_M^2/σ^2. Consequently, it is the purpose of this paper to investigate the properties of Eq. (2) for covariance functions which result from the application of white gaussian noise to first and second order systems. In doing this, we shall find that a significant advantage can be obtained if the sampling is performed at the output of a second-order system.

Finally, as an application of these results, the technique of sampling the automatic gain control (AGC) voltage for carrier signal power estimation will be examined. Accuracies available using the existing sampling procedure will be given and then compared with the accuracies attainable using the correlated sampling results.

Before proceeding, a comment regarding notation is in order. The ratio σ_M^2/σ^2 occurs quite often and hence will be designated by $\sigma_M^2/\sigma^2 = \lambda$. Whenever the limiting case (continuous sampling) of λ is considered, it will be identified by λ_∞ where

$$\lambda_\infty = \lim_{N\to\infty}\left\{\frac{\sigma_M^2}{\sigma^2}\right\}$$

$$T = Nt_0 = \text{constant}$$

Finally, it is important to note that when the properties of a function are illustrated graphically, it is often necessary to normalize the ordinate and/or abscissa. Since normalization constants may differ for different covariance functions, it is necessary to use caution when making quantitative comparisons.

II. Correlated Sampling in First-Order Systems

Consider a first-order system having a transfer function

$$F(s) = \frac{a}{s+a}$$

where a is a real constant greater than zero. If this system is disturbed by zero mean white gaussian noise having a two-sided spectral density of $N_0/2$ the resulting output covariance function will be

$$R(\tau) = \frac{N_0 a}{4}\cdot\exp(-a|\tau|)$$

$$= \sigma^2\cdot\widetilde{R}(\tau)$$

Substituting the normalized covariance function into Eq. (2) we obtain the relationship between λ, N and t.

$$\lambda = \frac{1}{N} + \frac{2}{N}\sum_{k=1}^{N-1}\left(1-\frac{k}{N}\right)\exp(-akt_0); \qquad t_0 \geqq 0 \qquad (3)$$

Equation (3) was evaluated numerically with the results given in Figs. 1a and 1b. Figure 1a represents the relationship between the total elapse sampling time $T = Nt_0$ and the sampling interval t_0 for various values of λ. For convenience of illustration both the ordinate and abscissa have been normalized by the reciprocal of a. In Fig. 1b we see the relationship between the required number of samples (N) and the normalized sampling interval (at_0).

Also shown in Figs. 1a and 1b are dashed lines corresponding to the independent sampling case when $\lambda = 0.05$. We see that both the elapse time and the required number of samples asymptotically approach the independent sampling case as the sampling interval increases. This is not surprising, since from Eq. (3), as t_0 becomes large the second term will die out, leaving

$$\lambda \approx \frac{1}{N}, \qquad t_0 \to \infty$$

Even more important is the fact that for all λ the total sampling time is a non-decreasing function of t_0. This implies that for each λ there corresponds a minimum elapse time (continuous sampling time) such that for any sampling duration less than this minimum time the corresponding λ cannot be achieved. To evaluate this minimum time, consider Eq. (2) with the substitution $N = T/t_0$. Taking the limit as N goes to infinity with T held constant yields

$$\lambda_\infty = \frac{2}{T}\int_0^T\left(1-\frac{t}{T}\right)\widetilde{R}(t)\,dt \qquad (4)$$

Substituting the normalized covariance function for the first-order system produces

$$\lambda_\infty = \frac{2}{aT} + \frac{2}{a^2T^2}(e^{-aT}-1)$$

$$\approx \frac{2}{aT}, \qquad \text{for } aT \text{ large} \qquad (5)$$

Equation (5) is illustrated in Fig. 1c where as before the elapse time has been normalized by the reciprocal of a.

III. Correlated Sampling in Second-Order System

Consider a second-order system having a transfer function

$$F(s) = \frac{ab}{(s+a)(s+b)}$$

Depending on the nature of the poles we see that there are three important cases for $F(s)$. Each of these will be considered separately.

A. Distinct Real Poles, $a > b > 0$

The covariance function for this system is given by

$$R(\tau) = \frac{N_0 ab}{4(a+b)} \cdot \frac{1}{1-z} \left[\exp(-b|\tau|) - ze^{-b|\tau|/z}\right] \quad (6)$$

where the substitution $z = b/a < 1$ has been made in the normalized covariance function of Eq. (6). The normalized portion of Eq. (6) is illustrated in Fig. 2 where the time axis has been normalized by the reciprocal of b.

As before, Eq. (2) is evaluated using this covariance function with the results shown in Fig. 3 for $z = \frac{1}{4}$. Figure 3a illustrates the relationship between the elapse time and sampling interval with both axes normalized by $1/b$. One of the independent sampling results is included for comparison.

As in the previous case the elapse time begins at some minimum value and increases asymptotically to the independent sampling result. The lower bound for the elapse time is given by

$$\lambda_\infty = \frac{2(1+z)}{bT} - \frac{2}{(bT)^2(1-z)}(1 - e^{-bT}) + \frac{2z^3}{(1-z)(bT)^2}(1 - e^{-bT/z}) \quad (7)$$

or as bT becomes large

$$\lambda_\infty \approx \frac{2(1+z)}{bT}$$

Equation (7) is illustrated in Fig. 3c with the time axis normalized by $1/b$.

B. Equal Real Poles $a = b > 0$

By exactly the same procedure as before one obtains

$$R(\tau) = \frac{N_0 a}{8} \cdot (1 + a|\tau|)\exp(-a|\tau|) \quad (8)$$

and

$$\lambda_\infty = \frac{4}{aT} + \frac{2}{aT}e^{-aT} - \frac{6}{(aT)^2}(1 - e^{-aT}) \quad (9)$$

with

$$\lambda_\infty \approx \frac{4}{aT}, \quad \text{for } aT \text{ large.}$$

Equation (8) is shown in Fig. 4. The results of the sample variance equation and a plot of Eq. (9) are given in Fig. 5. In both figures the time axes have been normalized by $1/a$.

C. Complex Conjugate Poles $a = \alpha + j\beta = b^*$

For this system the transfer function is

$$F(s) = \frac{\alpha^2 + \beta^2}{(s + \alpha + j\beta)(s + \alpha - j\beta)}$$

and the corresponding covariance function is given by

$$R(\tau) = \frac{N_0(\alpha^2 + \beta^2)}{8\alpha} \cdot e^{-\alpha|\tau|}\left(\cos \alpha z\tau + \frac{\sin \alpha z|\tau|}{z}\right) \quad (10)$$

where $z = \beta/\alpha$. Equation (10) is illustrated in Fig. 6 for z equals 1, 2, and 4 with the time axis normalized by the reciprocal of α.

For the first time we see a marked change in the structure of the covariance function. For certain regions of the time axis the covariance becomes negative. One would, therefore, expect the sampling performance to depart from the trends established in the previous cases.

By evaluating Eq. (2) with the normalized version of Eq. (10) one obtains the curves shown in Fig. 7. Figures 7a and 7b show only the case for $\lambda = 1/256$, but similar curves are obtained for other values of λ. The corresponding independent sampling result is also shown. The continuous sampling limit is determined from Eq. (4) to be

$$\lambda_\infty = \frac{4}{\alpha T(1+z^2)} - \frac{2(3-z^2)}{[\alpha T(1+z^2)]^2} + \frac{2e^{-\alpha T}\left\{(3-z^2)\cos \alpha zT + \frac{(1-3z^2)}{z}\sin \alpha zT\right\}}{[\alpha T(1+z^2)]^2} \quad (11)$$

and is shown in Fig. 7c. All the time axes of Fig. 7 are normalized by the reciprocal of α.

From Figs. 7a and 7b we see that the expected departure from the previous results did, in fact, occur. In the previous cases the sampling time approached the independent sampling result asymptotically from above. For the complex pole case, however, we see that for certain ranges of the sampling interval, the total time and re-

quired number of samples actually fall below the independent sampling result. Since the independent sampling result depends on λ and not on the system time constants, one can conclude that significant time savings can be achieved when sampling of second-order systems.

IV. Application to Carrier Power Estimation Accuracy

To see how the correlated sampling results can be applied, let us consider the sampling of the DSIF receiver AGC voltage for received carrier signal power estimation. The receiver AGC voltage is derived from a coherent amplitude detector and used to stabilize the output of a variable gain IF amplifier. The AGC voltage will, therefore, have some functional relationship with the received signal power. The DIS monitor computer samples this voltage with a sampling interval of 1.0 s and forms a sample mean of five samples. The sample mean is then applied to an approximate inverse functional to obtain an estimate of the received signal power.

Let us assume that the inverse functional is exact. It is desired to estimate the error in the signal power estimate due to the AGC sampling. To do this, the accuracy available using the existing sampling scheme will first be computed. Then the previous results will be applied to show how, in some cases, the accuracy can be improved. In both cases the receiver is assumed to have an operating noise temperature of 40 K and be configured for the narrow tracking loop bandwidth.

To compute the accuracy of the AGC sampling it is necessary to determine the variance of the AGC voltage. This can be done by using the results of Chapters 7 and 8 of Tausworthe (Ref. 2). Using Tausworthe's notation this variance is given by

$$\text{var}\,[c(t)] = \left[\left(\frac{20\log e}{eg}\right)^2\left(\frac{K}{A^*}\right)^2\frac{N_0W_c}{2} + 2\,(\log e\sigma_\phi^2)^2\frac{W_c}{W_1}\right]C^2(0) \qquad (12)$$

where K is the receiver gain. Values for W_1 and σ_ϕ^2 can be computed from Eqs. (8)–(13), (8)–(15), (8)–(17) and (8)–(18) of Tausworthe's report. The remaining entries can be computed from his Chapter 7.

In order to use Eq. (12), however, it is necessary that the log power gain of the variable IF amplifier be a linear function of the AGC voltage. Specifically, it is necessary that

$$20\log\left(\frac{1}{A^*}\right) = K_R' + K_A' C(t) \qquad (13)$$

A more accurate expression for this gain is

$$20\log\left(\frac{1}{A^*}\right) = 55.69 + 13.05\,C(t) + 1.006\,C^2(t) + 0.105\,C^3(t) \qquad (14)$$

However, Eq. (12) can still be used if Eq. (14) is linearized about its operating point. This was accomplished by computing the AGC voltage using the global approximate values $K_R' = 54$ dB and $K_A' = 12.2$ dB/V. Evaluating Eq. (14) and its derivative at this value of $C(t)$ results in new values for K_R' and K_A'. Upon substitution of these new values into Eq. (12) the desired variance was obtained. In addition a new value of $C(t)$ was computed using the updated values of K_R' and K_A' as a check. The results are illustrated in Table 1 for the narrow, medium, and wide AGC bandwidths.

The entries of Table 1 were also used to determine the 3σ accuracy of the carrier power (P_s) estimate by using a 12.2 dB/V conversion factor. These results are shown in Fig. 8.

Finally, note that the AGC circuit is essentially a first-order system. It would be interesting to see if some benefit could be obtained by converting this system (by means of a compensating filter) to an equivalent second-order system. For equivalence it is necessary that the output variance, or equivalently the noise bandwidths, of the two systems be identical. If the first-order transfer function is

$$H_1(s) = \frac{a}{s+a}$$

and the second-order transfer function is given by

$$H_2(s) = \frac{\alpha^2+\beta^2}{(s+\alpha+j\beta)(s+\alpha-j\beta)}$$

with $z = \beta/\alpha$, then the normalization constants used in *Subsections II* and *III* are related by

$$\alpha = \frac{2a}{z^2+1} \qquad (15)$$

Now, if we desire to know the elapse sampling time required to produce some 3σ power estimate accuracy (e.g.,

0.1 dB) we can use Eq. (2) with the appropriate covariance function and the relationship given in Eq. (15). Figure 9 illustrates the results for the three AGC bandwidths and a second-order parameter value $z = 4$. The first-order results are identified by a ① and the second order by ②. The solid vertical line depicts the set of all elapse sampling times less than or equal to 5 s and at a sampling interval of 1.0 s (the presently used sampling parameters).

It is clear from Fig. 9a that for a narrow AGC bandwidth it is more beneficial to sample from a first-order system. For the medium bandwidth, however, a significant decrease in elapse time can be obtained if the sampling is performed at the output of a second-order system. For example, if it is desired to estimate a power level of −155 dBmW with 0.1 dB accuracy, it is necessary only to double the sampling time. For the first-order system, however, a 4-to-1 increase is required. Finally, for the wide AGC bandwidth little benefit can be obtained from either system unless the sampling interval becomes quite small.

V. Conclusion

Contained herein is a set of curves relating the correlated sampling parameters for first- and second-order systems. Furthermore, it was noticed that for specific sampling intervals a significant improvement in both the sampling time and required number of samples can be achieved if the sampling is performed at the output of an equivalent second-order system. In particular, it was noticed that approximately a 2-to-1 improvement resulted when this technique was applied to the AGC sampling for the medium AGC bandwidth. This may be of some interest for the *Pioneer F* and *G* missions where it is anticipated that the medium AGC bandwith will be used.

References

1. Davenport, W. B., and Root, W. L., *Random Signals and Noise*, McGraw-Hill Book Co., Inc., New York, 1958.
2. Tausworthe, R. C., *Theory and Practical Design of Phase Locked Receivers*, Vol. I, Technical Report No. 32-819, Jet Propulsion Laboratory, Pasadena, Calif., February 1966.

Table 1. Computed values of AGC voltage mean and variance for narrow carrier tracking loop bandwidth and $T_{op} = 40\ K$

Received carrier power, dBmW	Average AGC, V	AGC variance, V^2		
		Narrow bandwidth	Medium bandwidth	Wide bandwidth
−110	−6.85	5.22×10^{-15}	5.84×10^{-14}	4.96×10^{-13}
−115	−6.39	5.22×10^{-14}	5.84×10^{-13}	4.96×10^{-12}
−120	−5.91	5.23×10^{-13}	5.85×10^{-12}	4.97×10^{-11}
−125	−5.35	5.27×10^{-12}	5.89×10^{-11}	5.01×10^{-10}
−130	−5.19	5.38×10^{-11}	6.01×10^{-10}	5.11×10^{-9}
−135	−4.64	5.71×10^{-10}	6.38×10^{-9}	5.43×10^{-8}
−140	−4.17	6.68×10^{-9}	7.46×10^{-8}	6.34×10^{-7}
−145	−3.71	8.89×10^{-8}	9.94×10^{-7}	8.44×10^{-6}
−150	−3.27	1.13×10^{-6}	1.26×10^{-5}	1.07×10^{-4}
−155	−2.84	1.06×10^{-5}	1.18×10^{-4}	1.00×10^{-3}
−160	−2.43	7.62×10^{-5}	8.52×10^{-4}	7.24×10^{-3}
−165	−2.07	4.96×10^{-4}	5.54×10^{-3}	4.71×10^{-2}
−170	−1.85	3.22×10^{-3}	3.60×10^{-2}	3.06×10^{-1}

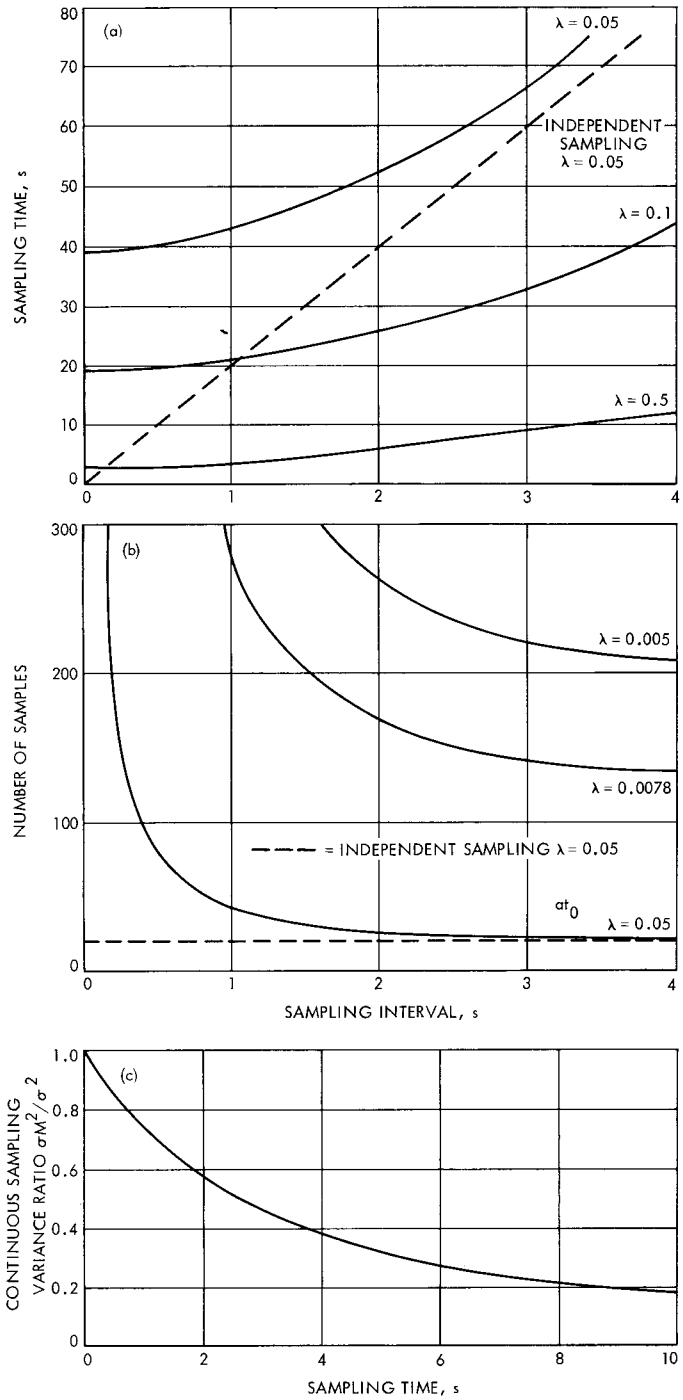

Fig. 1. Sampling performance for first-order system: (a) required sampling time, (b) required number of samples, (c) continuous sampling limit

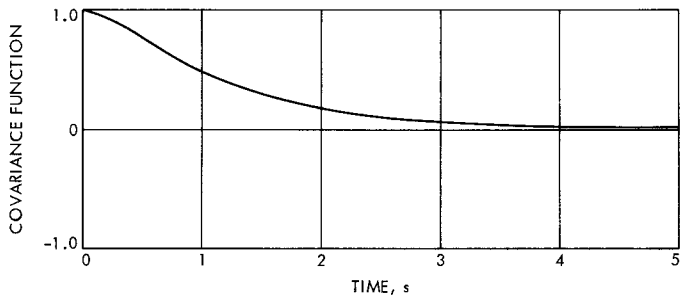

Fig. 2. Normalized covariance function of second-order system with distinct real poles and z = ¼

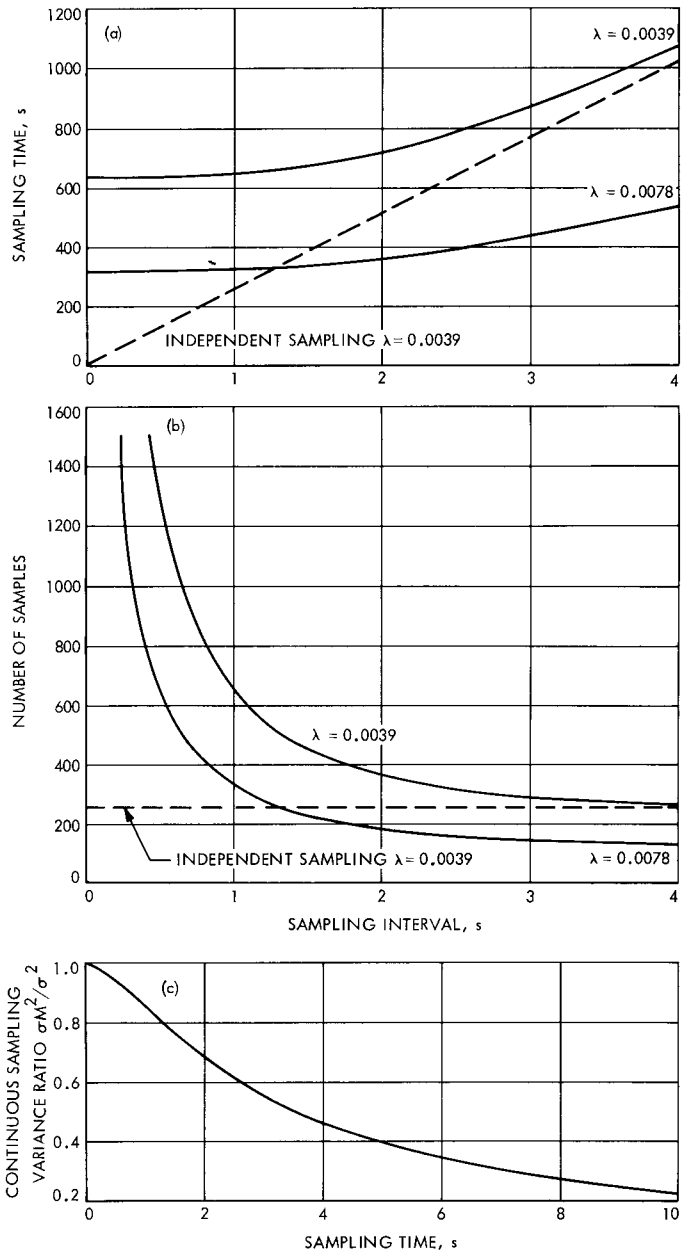

Fig. 3. Sampling performance for second-order system with distinct real poles and z = ¼: (a) required sampling time, (b) required number of samples, (c) continuous sampling limit

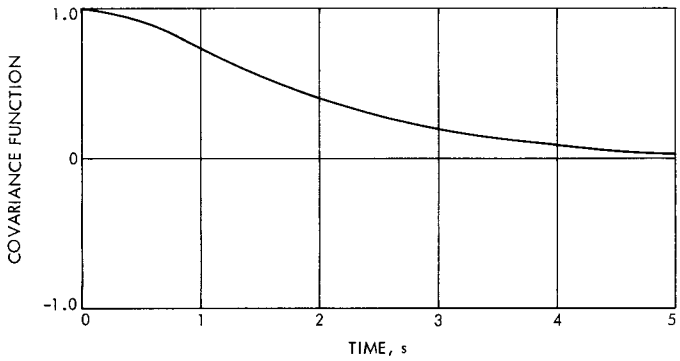

Fig. 4. Normalized covariance function for second-order system with equal real poles

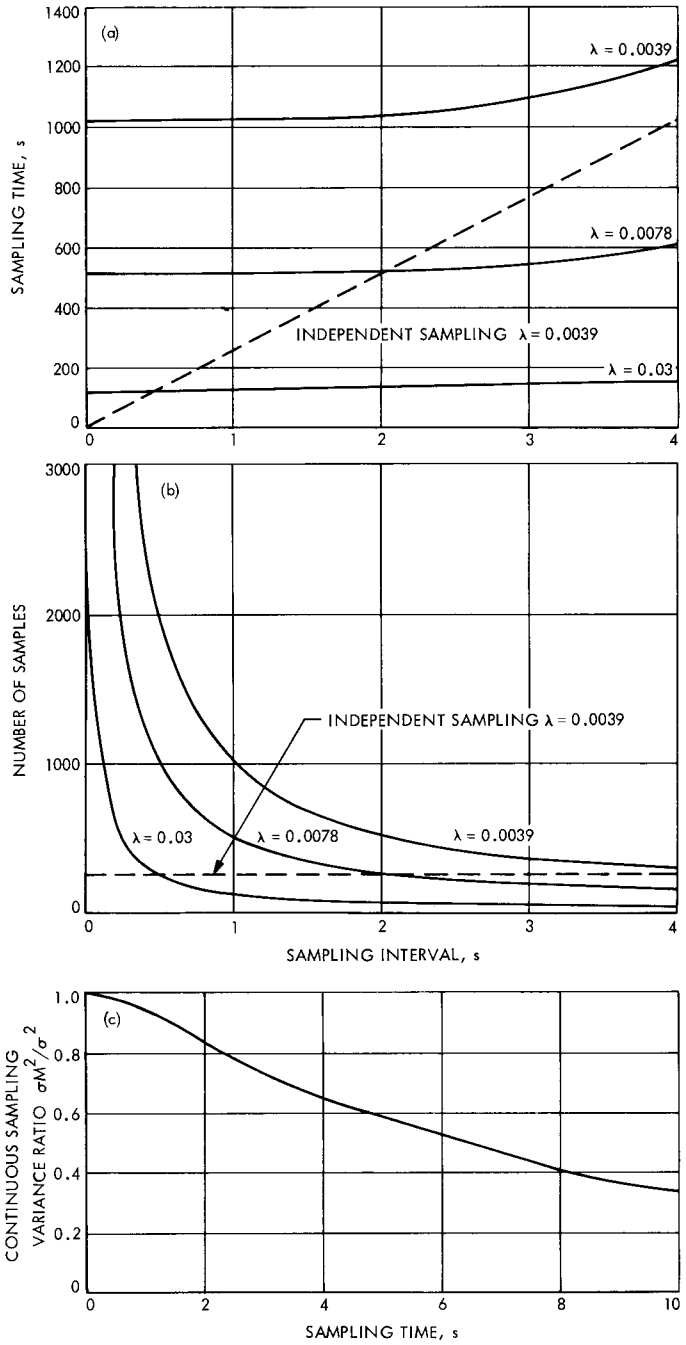

Fig. 5. Sampling performance for second-order system with equal real poles: (a) required sampling time, (b) required number of samples, (c) continuous sampling limit

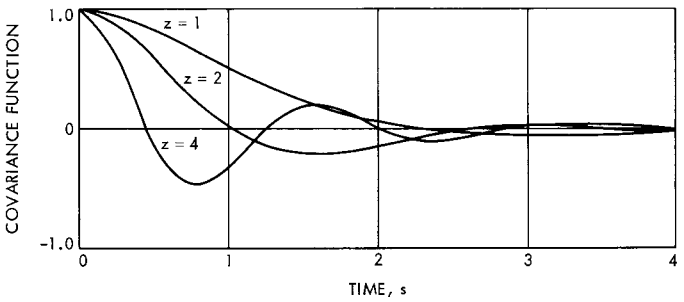

Fig. 6. Normalized covariance function for second-order system with complex conjugate poles

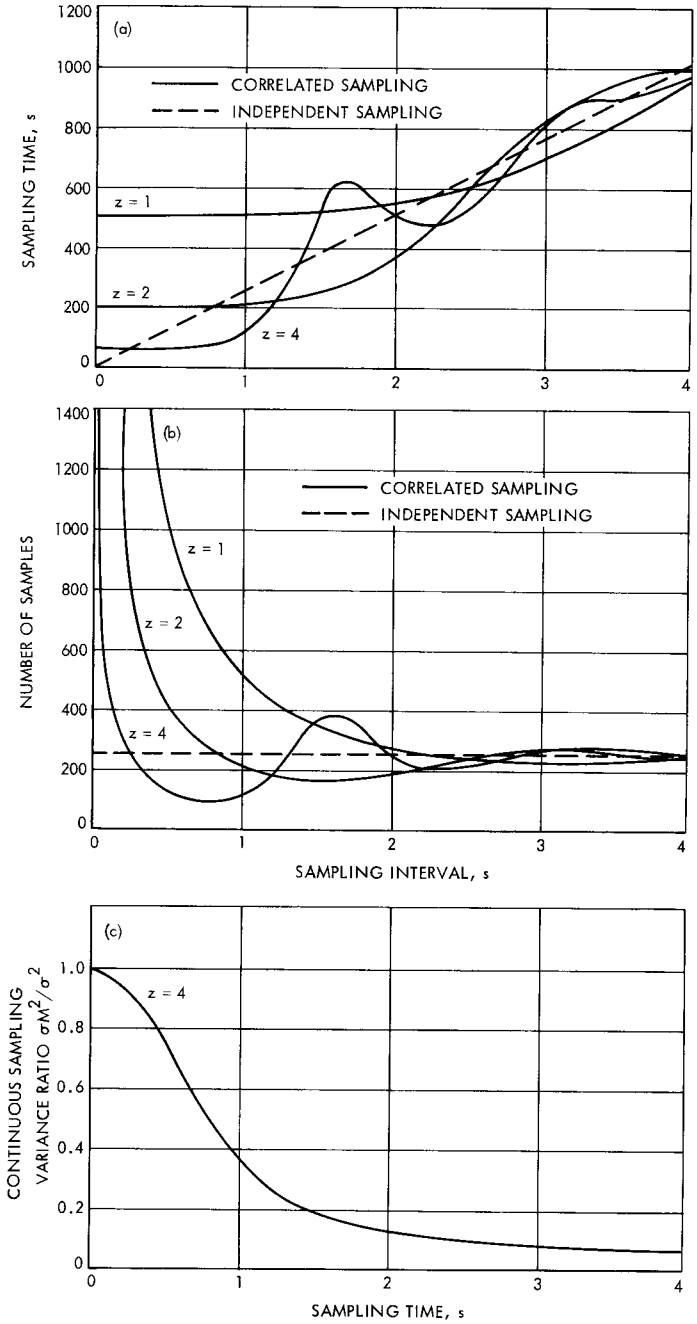

Fig. 7. Sampling performance for second-order system with complex conjugate poles: (a) required sampling time for $\lambda = 1/256$, (b) required number of samples for $\lambda = 1/256$, (c) continuous sampling limit

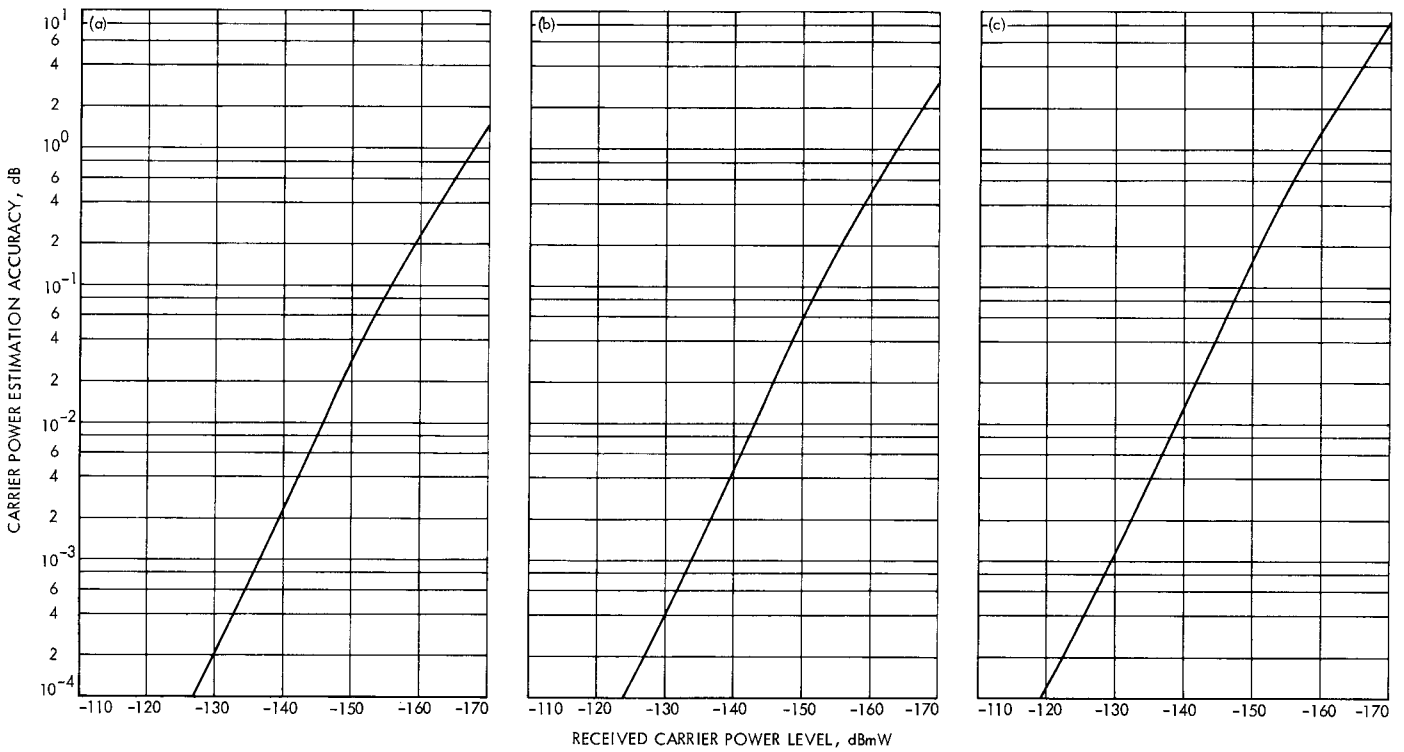

Fig. 8. Carrier power estimation accuracy using present sampling technique: (a) narrow AGC bandwidth, (b) medium AGC bandwidth, (c) wide AGC bandwidth

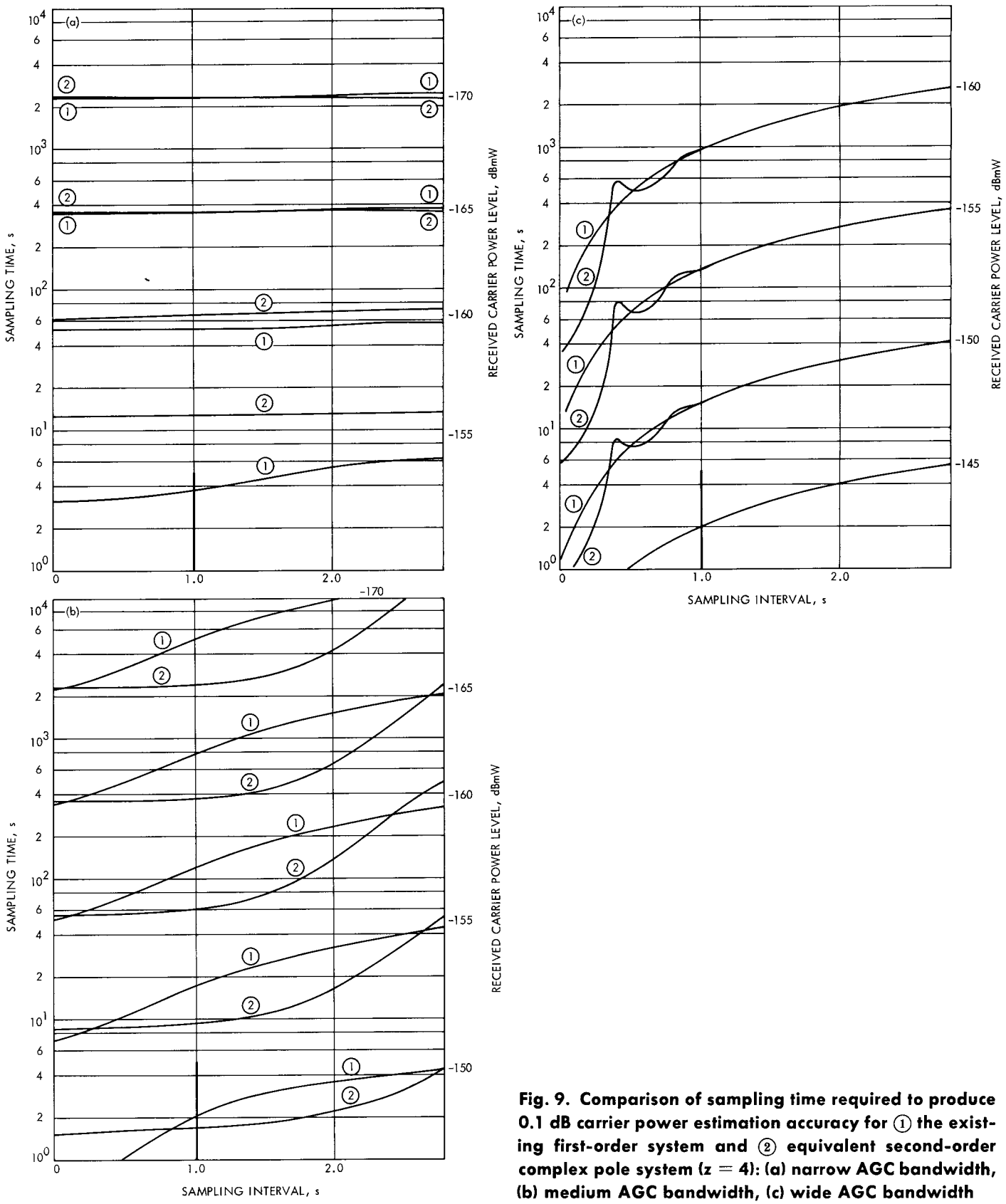

Fig. 9. Comparison of sampling time required to produce 0.1 dB carrier power estimation accuracy for ① the existing first-order system and ② equivalent second-order complex pole system (z = 4): (a) narrow AGC bandwidth, (b) medium AGC bandwidth, (c) wide AGC bandwidth